ARTICLE

Strong Overtones Modes in Inelastic Electron Tunneling Spectroscopy with Cross-Conjugated Molecules: A Prediction from Theory

Jacob Lykkebo,[†] Alessio Gagliardi,[‡] Alessandro Pecchia,[§] and Gemma C. Solomon[†,*]

[†]Nano-Science Center and Department of Chemistry, University of Copenhagen, Universitetsparken 5, 2100 Copenhagen Ø, Denmark, [‡]Department of Electronic Engineering, Università di Roma "Tor Vergata", Via del Politecnico 1, 00133 Rome, Italy, and [§]Consiglio Nazionale delle Ricerche, ISMN, Via Salaria km 29.6, 00017 Monterotondo, Rome, Italy

ABSTRACT Cross-conjugated molecules are known to exhibit destructive quantum interference, a property that has recently received considerable attention in single-molecule electronics. Destructive quantum interference can be understood as an antiresonance in the elastic transmission near the Fermi energy and leading to suppressed levels of elastic current. In most theoretical studies, only the elastic contributions to the current are taken into account. In this paper, we study the inelastic contributions to the current in cross-conjugated molecules and find that while the inelastic contribution to the current is larger than for molecules without interference, the overall behavior of the molecule is still dominated by the quantum interference feature. Second, an ongoing challenge for single molecule electronics is understanding and controlling the local geometry at the molecule-surface interface. With this in mind, we investigate a spectroscopic method capable of providing insight into these junctions for cross-conjugated molecules: inelastic electron tunneling spectroscopy (IETS). IETS has the advantage that the molecule interface is probed directly by the tunneling current. Previously, it has been thought that overtones are not observable in IETS. Here, overtones are predicted to be strong and, in some cases, the dominant spectroscopic features. We study the origin of the overtones and find that the interference features in these molecules are the key ingredient. The interference feature is a property of the transmission channels of the π system only, and consequently, in the vicinity of the interference feature, the transmission channels of the σ system and the π system become equally transmissive. This allows for scattering between the different transmission channels, which serves as a pathway to bypass the interference feature. A simple model calculation is able to reproduce the results obtained from atomistic calculations, and we use this to interpret these findings.

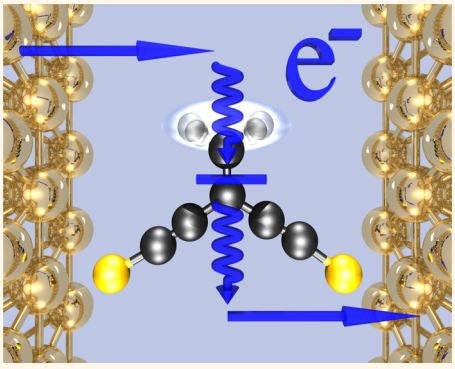

KEYWORDS: inelastic electron tunneling spectroscopy · quantum interference · molecular electronics

As the continued downscaling of components in classical electronic devices reaches its limitations, the idea of a bottom up approach where single molecules are self-assembled into logical circuits becomes increasingly interesting. Molecules that exhibit destructive quantum interference effects are promising in this context. Destructive quantum interference has recently been observed experimentally, directly[1] and indirectly,[2,3] in molecular junctions and is receiving considerable attention due to the intriguing physics involved and the potential for possible applications in single-molecule electronics.[4] Destructive quantum interference can be understood theoretically as an antiresonance in the transmission and results in suppressed levels of elastic current. The inelastic contributions to the current have, to the best of our knowledge, not been studied.

A major challenge in single-molecule electronics is the inability to study the geometry of the junction directly. As a result, the models used for the geometries of the single-molecule junctions are often nothing but idealizations; for example, electrodes are depicted as perfect flat surfaces or small pyramids with the molecule standing perpendicular to the surface. The discrepancy between the actual geometry and the idealization can lead to problems for

* Address correspondence to gsolomon@nano.ku.dk.

Received for review July 22, 2013 and accepted September 19, 2013.

Published online September 19, 2013
10.1021/nn4037915

interpretation. An example of this is in the pioneering work by Reed *et al.*[5] where the conductance of a single benzene-dithiol molecule in a gold junction was measured for the first time. In subsequent theoretical studies of this junction, the atomistic geometry used for the gold−molecule−gold interface was, for lack of better alternative, a simplified geometry.[6,7] While the proposed structure seemed reasonable, there was no actual evidence behind it, and subsequent theoretical studies have suggested that alternative orientations for the molecule,[8,9] interactions between different molecules in the junctions[10] or the gold molecule interface[11,12] might be considerably more complicated. In this case, it led to a measured conductance that was an order of magnitude lower than the theoretically predicted value, and thus illustrates the necessity to understand the details of the junction geometry. The chemists' answer to such a problem is that we need spectroscopic methods to characterize these junctions.

One promising spectroscopic method to study a molecular junction *in situ* is to use inelastic electron tunneling spectroscopy (IETS). In IETS, the vibrational spectrum of the molecule, or monolayer in a junction, is obtained by passing current through the system. Unlike other vibrational spectroscopies, such as Raman or IR, the vibrational spectrum is obtained directly from the current, thereby unambiguously probing the geometry of the junction under bias, while assuring that the current/voltage and the vibrational spectra are obtained from the same part of the system.

Another interesting feature of IETS is that it can yield signatures that are forbidden in other vibrational spectroscopies such as Raman or IR. Furthermore, since IETS utilizes the current to excite the vibrational modes, it has the potential to unambiguously provide knowledge of the local geometry in a single molecule junction, since the inelastic electron tunneling (IET) spectra are strongly dependent on the molecular geometry.[8,13] While the method itself is fairly old,[14] its use is not widespread. However, studies of IETS on monolayers[15,16] and single molecules[17−19] have been published, making it more common in recent years.

One defining characteristic of IETS, compared with other vibrational spectroscopies, is the lack of definite selection rules, since the incident current has components of all symmetries of the system.[20] Instead, the peaks are determined by the weaker propensity rules. Thus, IETS is an excellent supplement to IR and Raman spectroscopy in high symmetry molecules, where many modes are forbidden.[21] This lack of selection rules poses problems when it comes to interpreting the spectra, and usually the peaks are assigned by comparing with Raman or IR spectra.[22]

Recently, there have been significant efforts to understand these propensity rules in IETS theoretically,[20,23−25] and a rule of thumb seems to be that the spectrum is *dominated by symmetric modes in the main tunneling path*.[23,24] Furthermore, the theoretical treatment of IETS can be used to assist in assignment of the experimental peaks, with a reasonable accuracy,[26−28] indicating that the computational treatment of IETS is sound.

Apart from the lack of hard selection rules, another defining property of IETS is that overtone modes are generally thought not to exist. This stems from both theoretical[29] and experimental (empirical)[22] evidence. As a result, many theoretical studies regarding IETS excluded the overtones by definition.[20,23,24,26,27]

In this paper we wish to study the inelastic contributions to the current of two different cross-conjugated molecules where quantum interference is known to exist (see Figure 1). The aim of this study is 2-fold. We wish to study if the quantum interference effect observed for the elastic transport is preserved when inelastic effects are included, and how large the proportion of the inelastic current is compared with the total current. Second, we wish to study the IET spectra of these molecules. Since the transport properties of molecules that exhibit quantum interference differs significantly from that calculated for ordinary conjugated molecules, the inelastic properties might differ significantly as well. For linearly conjugated molecules, the elastic transport is high, so the inelastic current can only add small contributions on top of a large elastic signal. For molecules with interference, the elastic current is suppressed allowing inelastic processes to be significantly more important. The basic premise is outlined in Figure 1A,B.

Although overtones are generally thought not to exist in IETS, in this paper we observe overtones for both cross-conjugated molecules considered. We aim to show that overtones in IETS may be common in this class of molecules. Quantum interference is shown to be critical to the observation of overtone modes. Cross-conjugated molecules have received relatively little attention until a few years ago,[30−32] and to the best of our knowledge, IETS has not yet been performed on these molecules, offering an explanation as to why overtones have not yet been observed in IETS.

Before we proceed, we would like to make a final introductory note regarding notation. Throughout this paper, we will refer to the electron−phonon coupling and phonons in the molecule, as this is the language commonly used to describe inelastic scattering in molecular junctions. The reader should note, however, that we calculate vibrational modes in the molecule (in a frozen gold junction) rather than propagating phonon modes in some large crystal. It remains an open question what influence phonon modes in the electrodes might have on these types of systems.

Introducing the Molecules. The systems used in this study are shown in Figure 1 and consist of two pairs of molecules. First, a meta- (MB) and a para-coupled

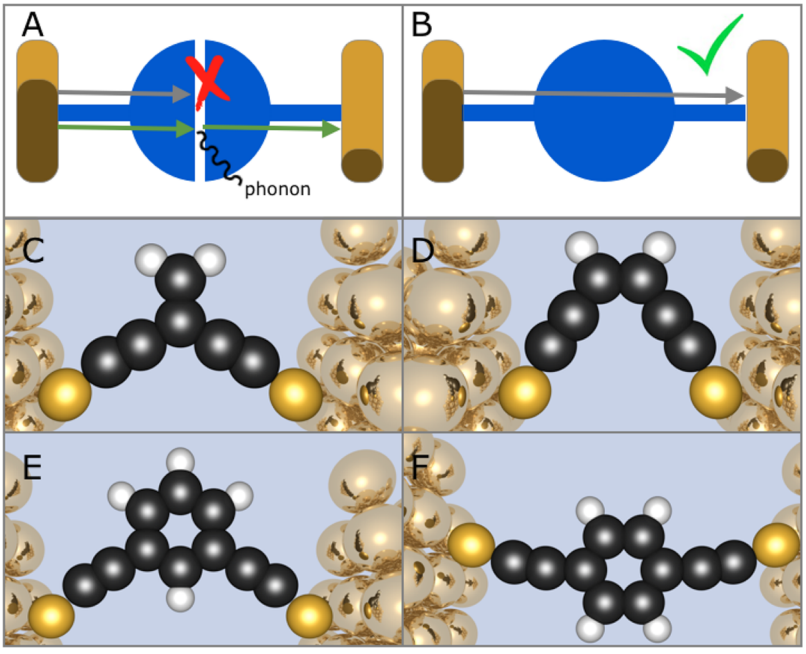

Figure 1. (A,B) A schematic of a molecule with (A) and without (B) destructive interference. For the molecule with interference the elastic current is effectively blocked, so that the inelastic contributions to the current become important. (C–F) The geometries of the four molecules in this study. For molecules with destructive quantum interference, the elastic current is effectively blocked, illustrated by the gray arrow. This allows the inelastic contributions to the current carried by vibrations to become important, illustrated by the green arrow. The molecules CC (C) and MB (E) are cross-conjugated, and the molecules LC (D) and PB (F) are linearly conjugated.

benzene ring (PB) and, second, a cross- (CC) and linearly coupled molecule (LC). The molecules are coupled to the electrodes *via* a thiolated triple bond linker, in order to bind to gold surface. The triple bonds are included in order to ensure that the current flows exclusively in and out through the thiols rather than through a possible short circuit with some other pathway through the central element.

The elements in each pair (CC and LC; MB and PB) are very similar; they contain the same number of atoms and have a very similar binding geometry, but their properties in a junction differ dramatically. CC is an acyclic cross-conjugated molecule where the two thiol groups are strongly coupled to each electrode and conjugated into the central part of the molecule but are nevertheless not conjugated to each other.[33] The MB is also a cross-conjugated system; the two thiol groups are each conjugated into the central benzene ring. However, because of the nature of the cyclic system, the conjugation does not extend from one thiol group to the other. As a result CC and MB have quite similar transport properties. LC and PB are linearly conjugated. All four molecules in the junction have C_s symmetry.[34]

Inelastic Electron Tunneling: A Conceptual Framework. When applying a finite bias across a molecular junction, a current will start to flow, and the electrons will tunnel across the molecular bridge either elastically or inelastically. Elastic tunneling is the process by which no energy is exchanged with the molecular bridge and the molecule acts simply as a tunneling barrier. In the low bias limit, the current is approximately linear as a function of the bias voltage. Inelastic tunneling, on the other hand, happens when the applied bias equals or exceeds the energy of a vibrational mode, q, of the molecule, such that $eV_{bias} \geq h\nu_q$. In this case, a quantum of energy, $E_q = h\nu_q$, can be transferred into the vibrational mode. This process opens up an additional inelastic channel for the current giving rise to a kink in the $I(V)$ spectrum that, when differentiated twice, gives rise to a peak in the $(d^2I)/(dV^2)(V)$ spectrum, which is defined as the IET spectrum. The process is schematically shown in Figure 2.

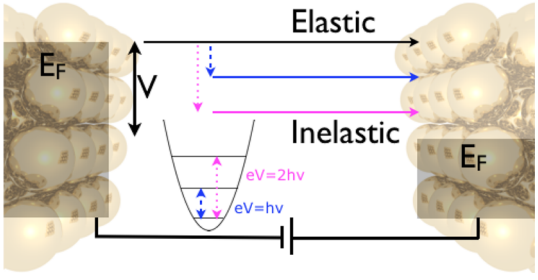

Figure 2. Schematic of the elastic and inelastic tunneling processes. The shaded areas on the left and right side denote the Fermi levels of the two electrodes under bias. Because of the applied bias, V, a current will flow. The current flows either elastically or inelastically, exciting once or twice a vibrational mode of the molecule thereby emitting energy that is absorbed by the molecule.

In order to calculate the IET spectra, the current is calculated using the Meir-Wingreen equation.[35] The inelastic scattering is introduced *via* the kinetic

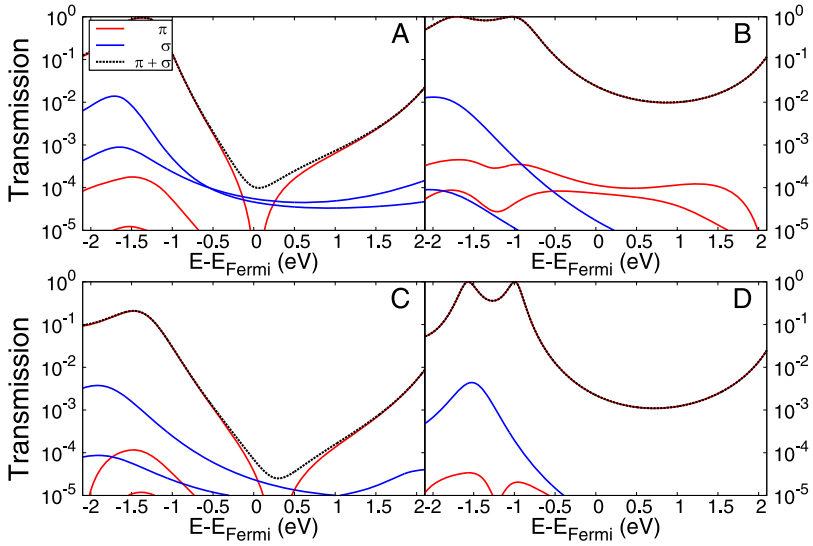

Figure 3. Transmission functions separated into σ and π transmission channels for CC (A), LC (B), MB (C), and PB (D). The cross-conjugated molecules show an interference feature near the Fermi energy. As a result, the σ transmission and the π transmission are similar in magnitude. For the linearly conjugated molecules, the transmission is completely dominated by the π transmission.

equations, which are expanded up to third order. In principle this allows for fundamental, overtone and second overtone processes. For full description of the theory, please consult the Supporting Information. Discarding the terms that do not contribute to the current (and thus the IET spectrum) and separating the terms into first- and second-order processes, the following qualitative picture is obtained for the first-order process:

$$\text{elastic channel in} \rightarrow \text{scattering} \rightarrow \text{elastic channel out}^{-} \quad (1)$$

and for the second-order process:

$$\text{elastic channel in} \rightarrow \text{scattering} \rightarrow \text{virtual state}^{-} \rightarrow \text{scattering} \rightarrow \text{elastic channel out}^{--} \quad (2)$$

where the $-$ ($--$) indicate that the energy has been shifted down by energy ω_q ($2\omega_q$), *i.e.*, the energy that is transferred into the vibrational mode q. The processes can, in principle, be extended to infinite order, but in the present study only the first- and second-order processes are found to be relevant (see Figure S4 in the Supporting Information, where higher order scattering processes are included for comparison). The virtual state in the middle is a retarded/advanced Green's function, which can be interpreted as propagation on the molecule before the second scattering event.

The second-order processes can, in principle, consist of both overtone modes, where the same vibrational mode is excited twice, and combination modes where two different vibrational modes are excited, but in the present study only the overtone mode processes are observed. The processes are illustrated in Figure 2. The method is similar to previous studies.[20,26] In this paper, only excitation processes are taken into account, since IET spectra are only obtained at cryogenic temperatures because of the large amounts of thermal noise at higher temperatures.[15] The molecules are therefore assumed to be in the vibrational ground state, and phonon absorption processes by charge carriers can be neglected.

RESULTS

gDFTB. The elastic transmission for the four molecules is shown in Figure 3. The transmission is split up into the σ and the π transmission components, which are defined with respect to the mirror plane in the molecular junction.[7,34] It should be noted that the σ transmission also contains the "in-plane" π orbitals of the triple bond linker. Hence, a more fitting name should perhaps be symmetric and asymmetric transmission, but in order to keep the notation simple and to maintain the intuition from elementary chemistry, the terms σ and π are used.

As seen in previous theoretical studies, the linearly conjugated molecules LC and PB are completely dominated by the π transmission near the Fermi energy, with the σ transmission several orders of magnitude less transmissive. For the cross-conjugated molecules CC and MB, there is an interference feature in the π transmission near the Fermi energy. Thus, the total transmission near the Fermi energy is dominated by the σ transmission or by a sum of the σ and the π transmission components. The results are well-known from previous theoretical studies[30−32,36] and supported by experimental observations.[1,3,37,38]

The inelastic contributions to the total current are found to be significantly larger for the cross-conjugated molecules compared with the linearly conjugated molecules. The results are summarized in Table 1. It is well-known that density functional theory

predicts band gaps that are too small compared with experiment, causing the predicted magnitudes of the current to be too large. Thus, the numbers presented in the table are simply indicative of the trends. It may be desirable to use cross-conjugation in designing molecules for use in IETS since the inelastic contributions to the current might be more easily observed.

We note that while the inelastic contributions to the current are larger than for the linearly conjugated analogues, the cross-conjugated systems are still clearly distinct, and the total current is found to be more than an order of magnitude lower that that for the linearly conjugated counterparts.

TABLE 1. Total Currents and % Inelastic Current[a]

molecule	total current (A)	% inelastic
CC	3.28×10^{-4}	55.3
LC	3.05×10^{-2}	14.8
MB	1.12×10^{-4}	47.2
PB	2.91×10^{-3}	15.6

[a] Cross-conjugation causes the total current to be an order of magnitude lower than the corresponding linearly conjugated molecule, because of quantum interference effects. The proportion of the current from inelastic pathways are significantly larger for cross-conjugated molecules compared to the corresponding linearly conjugated molecules. The applied bias is 0.45 eV.

One major drawback of IETS is the relatively low resolution of the spectra. Broadening due to thermal fluctuations requires that the spectra are obtained at cryogenic temperatures.[15] Furthermore, even at low temperatures, the peaks are generally broad, and only the stronger modes in the spectra are easily distinguished. This stems partly from the fact that a relatively small fraction of the total current is inelastic[39] so that the signatures of the inelastic current are small variations on top of a large elastic signal.

In order to increase the resolution of IETS, it should be possible to design molecules where the inelastic to elastic ratio of the current is large. These molecules might be able to aid in the study of the geometry of a molecular junction or during pulling experiments.[40,41]

The calculated IET spectra are shown in Figure 4 with the positions of the phonon frequencies and the overtone phonon frequencies (twice the phonon frequency) indicated with blue circles and red triangles, respectively. For the two molecules CC and MB, strong overtones are observed at ~0.2 eV. The insets in Figure 4A,C show the IET spectrum with only the single vibrational mode that is responsible for the overtone included. It is clear that these single vibrational modes result in two peaks in the IET spectra. For some of the vibrational modes, the overtone is found to be larger

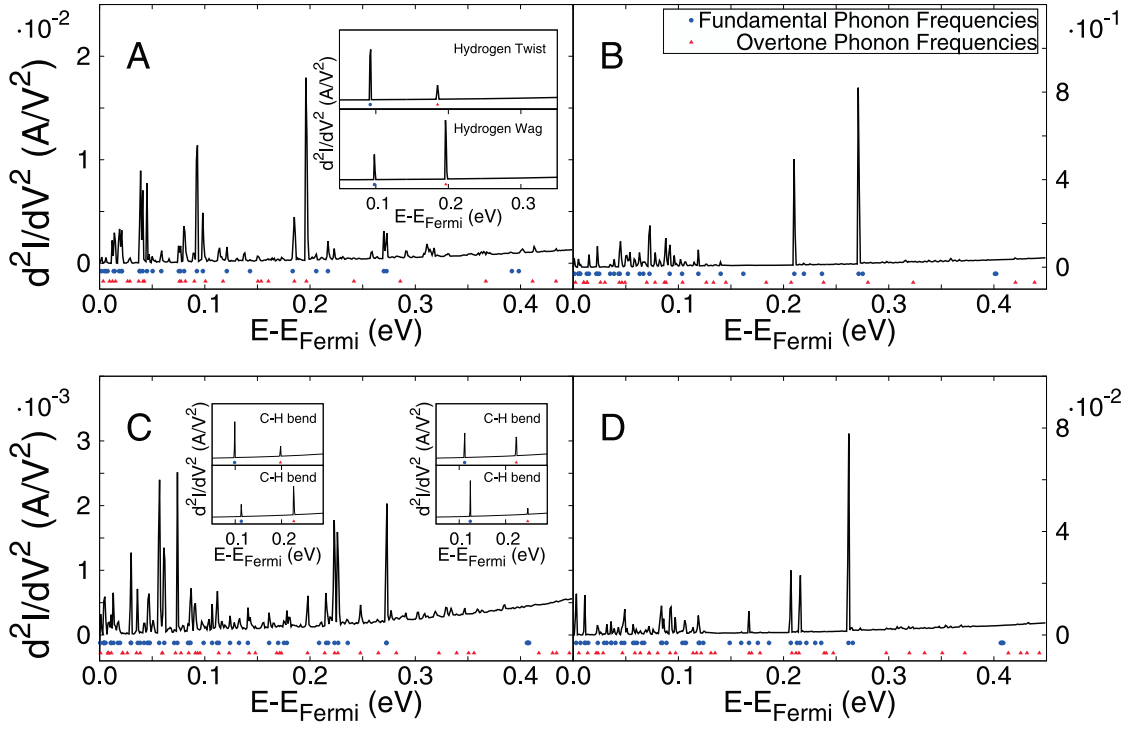

Figure 4. IET spectra of CC (A), LC (B), MB (C), and PB (D). The positions of the phonon frequencies are indicated by the blue dots for the fundamental modes and the red triangles for the overtone modes. The insets show calculations of IETS including only a single vibrational mode illustrating that one vibrational mode gives rise to two peaks in the IET spectrum. The vibrational modes in the insets of MB are the four asymmetric hydrogen modes. For the linearly conjugated molecules, the main vibrational modes are found to be the stretch modes of the double and triple bonds. For the cross-conjugated molecules, the main vibrational modes are found to be asymmetric vibrational modes. Furthermore, overtones are observed for both of the cross-conjugated molecules, and these overtone modes stem from allowed vibrational modes, but are nevertheless found to be dominant in these cases.

than the fundamental mode. We note that, in all cases, the second overtone is not present for any of the vibrational modes. Furthermore, the individual elements of the electron−phonon coupling matrices are similar in magnitude irrespective of whether they give rise to an overtone or not. All these results indicate that the computational treatment is sound and that the overtones are not an artifact of the computational method, such as a breakdown in the theory due to a large electron−phonon coupling.[42]

The vibrational modes responsible for the overtones in both CC and MB are found to be asymmetric vibrational modes of the hydrogens with respect to the mirror plane of the molecules. Thus, four strong overtones for MB and two for CC are observed (corresponding to the number of hydrogen atoms in these two systems). Indeed, for both cross-conjugated molecules most of the main features in the IET spectra stem from asymmetric vibrational modes. For CC, two of the three closely spaced peaks located at ∼0.045 eV are due to asymmetric vibrational modes, whereas the last is due to a symmetric mode. All three are related to the vibrations of the carbon backbone with the main vibrational motion located on the triple bond. Of the three strong peaks in the IET spectrum between 0.05 and 0.08 eV of MB, the two largest at ∼0.051 and ∼0.07 eV are due to asymmetric vibrational modes, while the third largest peak at ∼0.053 eV is due to a symmetric vibrational mode. The other dominant modes in the IET spectra for CC and MB are the symmetric triple bond stretch at ∼0.27 eV. For both cross-conjugated molecules, the dominant modes in the IET spectrum are thus the asymmetric modes, and consequently the most important scattering processes are those where the in and the out channels have different symmetries.

The C═C double bond stretch in CC is located at ∼0.22 eV and is found to be a very weak mode. This mode would be predicted to be an important mode if we draw an analogy between this system and a stub resonator, which is well-known in condensed matter nanoelectronics.[43] In a stub resonator, quantum interference effects are know to arise when the energies of the incoming wave match the energy of a bound state of the stub. Changing the depth of the stub will change the interference effects by changing the energy of the bound state. Thus, it could be expected that the vibrational mode of the C═C double bond stretch in CC and the incoming wave could strongly interact due to the modulation of the stub; however, this is not the case. Similarly, if one argued that the interference in CC stems from two tunneling paths, one where the electron passes straight through the system and one where it takes a detour through the side arm, the conclusion would be that this mode should be able to modulate the interference effect. At this level of treatment, however, it is found to be unimportant. In fact, it seems that the understanding of which of the vibrational modes are important must be gained from chemical intuition, rather than from topological reasoning.

TABLE 2. Description of the Significant Vibrational Modes Observed in the IET Spectra, Indication Whether the Modes Are Symmetric (S) or Asymmetric (A), and the Dominant Scattering Process for the Modes[a]

molecule	description of mode	energy (eV)	symmetry	dominant scattering processes
CC	center of mass	0.038	S	$\sigma \rightarrow \sigma$
CC	center of mass	0.041	A	$\sigma \rightarrow \pi, \pi \rightarrow \sigma$
CC	center of mass	0.045	A	$\sigma \rightarrow \pi, \pi \rightarrow \sigma$
CC	hydrogen wag	0.093	A	$\sigma \rightarrow \pi, \pi \rightarrow \sigma$
CC	overtone hydrogen wag	0.186	A	$\pi \rightarrow \sigma \rightarrow \pi$
CC	hydrogen twist	0.098	A	$\sigma \rightarrow \pi, \pi \rightarrow \sigma$
CC	overtone hydrogen twist	0.196	A	$\pi \rightarrow \sigma \rightarrow \pi$
LC	C═C stretch	0.211	S	$\pi \rightarrow \pi$
LC	C≡C stretch	0.272	S	$\pi \rightarrow \pi$
MB	center of mass	0.057	A	$\sigma \rightarrow \pi, \pi \rightarrow \sigma$
MB	center of mass	0.062	S	$\pi \rightarrow \pi$
MB	center of mass	0.074	A	$\sigma \rightarrow \pi, \pi \rightarrow \sigma$
MB	CH bend in benzene ring	0.087	A	$\sigma \rightarrow \pi, \pi \rightarrow \sigma$
MB	overtone of CH bend	0.174	A	$\pi \rightarrow \sigma \rightarrow \pi$
MB	CH bend in benzene ring	0.099	A	$\sigma \rightarrow \pi, \pi \rightarrow \sigma$
MB	overtone of CH bend	0.199	A	$\pi \rightarrow \sigma \rightarrow \pi$
MB	CH bend in benzene ring	0.112	A	$\sigma \rightarrow \pi, \pi \rightarrow \sigma$
MB	overtone of CH bend	0.224	A	$\pi \rightarrow \sigma \rightarrow \pi$
MB	CH bend in benzene ring	0.113	A	$\sigma \rightarrow \pi, \pi \rightarrow \sigma$
MB	overtone of CH bend	0.226	A	$\pi \rightarrow \sigma \rightarrow \pi$
MB	C≡C stretch	0.273	S	$\pi \rightarrow \pi$
PB	ring stretch	0.207	S	$\pi \rightarrow \pi$
PB	ring stretch	0.215	S	$\pi \rightarrow \pi$
PB	C≡C stretch	0.262	S	$\pi \rightarrow \pi$

[a] The low energy vibrational modes involving several atoms are labelled Center of Mass and are described in the text.

In the two linearly conjugated molecules, the important scattering processes are fundamentally different from those observed for the cross-conjugated systems. First, there are significantly fewer features in the IET spectra, with only two and three significant peaks in the spectrum of LC and PB respectively. Second, the dominant modes are due to symmetric vibrational modes. For CC, the dominant features are due to the triple and double bond stretches at ∼0.21 and ∼0.27 eV. For PB, it is the triple bond stretch at ∼0.26 eV and the C−C stretches in the benzene ring at ∼0.207 and ∼0.215 eV that give rise to the main features. It is mainly the longitudinal vibrational modes that are responsible for the inelastic scattering in the linearly conjugated molecules. This observation follows the propensity rules discussed previously by Troisi and Ratner[23,24] and by Gagliardi *et al.*[20] The main vibrational modes are collected in Table 2.

In order to understand why the strong stretch modes observed in LC are not observed for the CC molecule, it is necessary to study the transmission channels of the molecule. The channels are shown in

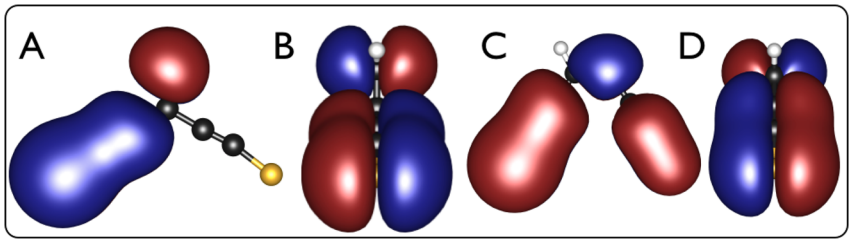

Figure 5. The most transmissive π-channel of CC (A and B) and LC (C and D) are shown from two angles. The channels are plotted at $E - E_{Fermi}$ = 0.004 eV, the energy at which the quantum interference in CC is centered. The asymmetry of the π-channels with respect to the mirror plane can be seen in B and D.

Figure 5 for CC and LC and are plotted at the energy of the interference feature ($E - E_{Fermi}$ = 0.004 eV). The transmission channels are obtained by diagonalizing the matrix product $A_L = G^a\mathbf{\Sigma}_L G^r$,[20] and can be interpreted as the scattering state through which the current can flow. The elastic transmission is then given by $\mathrm{Tr}[A_L\mathbf{\Gamma}_R]$, which describes how the transmission channel is coupled to the right electrode. The inelastic transmissions, T_{inc}, for the fundamental and overtone modes are then obtained from expressions similar to eqs 1 and 2, respectively. The equations are given in the Supporting Information in eqs S14 and S15. For LC, where the transmission is dominated by a single π-channel, the channel density is observed to decay along the length of the molecule. This illustrates how the transmission of linearly conjugated molecules falls off exponentially as a function of the length of the molecule.[44] For CC on the other hand, the π-channel is dramatically affected by the interference feature. It is observed that the channel density is high from the left electrode and into the central part of the molecule, but on the right side of the molecule the channel density is completely suppressed. Indeed, the channel density of the carbon immediately to the right of the central part of CC is 2000 times lower than the density of the carbon atom immediately to the left of the central part. The high channel density on the left side of CC and the very low density on the right-hand side illustrate the fact that the molecule is fully conjugated from the electrodes and into the central part of the molecule but not from the left electrode to the right electrode.

The overall appearance of the channels are, in general, independent of energy. An exception to this is the right-hand side of CC, where small channel densities appear on the right-hand side of the molecule as the energy is shifted slightly away from the interference feature. Thus, the strong triple bond stretch modes, which are present in the linearly conjugated molecules, are strongly repressed in the CC molecules due to the small overlap between the in- and the out-channels, but since the vibrational modes are shifted slightly away from the interference feature, the stretches are not completely suppressed. The double bond stretch, on the other hand, is located well within the overlap of the in- and the out-channels but is instead suppressed since the transmission channel has a node exactly on the central carbon atom.

The phonon frequencies for the carbon−hydrogen stretches are located at ∼0.4 eV for all four molecules, and for all molecules the associated peaks in the IET spectra are found to be very small. The hydrogen stretches are found to be the dominant mode in recent IETS studies on self-assembled monolayers[16,45] and in electromigrated nano gaps,[46] whereas other studies find them to be less significant.[15] A recent combined theoretical and experimental study of monolayers of alkanemonothiols found that both the CH_3 and the CH_2 groups contribute to the hydrogen stretch feature in the IET spectrum.[45] The large peak is observed experimentally but not seen in the calculations, and it is speculated that hydrogen stretches are due to intermolecular interactions and are therefore significantly smaller in computational studies where only a single molecule is treated. Another theoretical study was able to reproduce the strong hydrogen stretches by tilting the molecule relative to the normal of the electrode surface.[13] It is, at present, uncertain whether these stretch modes are missing in the calculations because of an error in the computational treatment or because of inconsistencies in the molecular geometry. At any rate, the hydrogen stretches are not important for the present study.

In order to study the scattering processes in more detail, the method of ref 20 is followed, but in this study it is also extended to allow us to understand the processes behind the overtones. Since the systems are all C_s symmetric, the matrices can be block diagonalized so as to separate the σ- and the π-system. Thus, the symmetry adapted scattering processes can be resolved. The symmetry adapted plots are shown in Supporting Information Figure S1. This allows the main scattering process for each of the modes in the spectrum to be determined. For the linearly conjugated molecules, the dominant processes are the π-in to π-out processes. This corresponds well with the intuitive understanding that the current mainly travels through the linearly conjugated molecules in the π-system, given that the π-channel completely dominates the elastic transmission. For CC and MB on the other hand, it is found that the dominant inelastic processes are the asymmetric σ- to π-processes involving an asymmetric vibrational mode.

Because of the interference feature in the π-transmission, the σ- and the π-transmission channels are equally transmissive, and thus scattering between the two channels is both symmetrically allowed and favored.

For the overtones, it is found that the dominant scattering processes are ones where both the in- and the out-channel are π, and where the virtual state in the middle is "σ".[47] Since the asymmetric vibrational modes scatter the current from channels of one symmetry to the other, the only allowed scattering processes for the overtones are the scattering processes σ-in $\rightarrow G_\pi \rightarrow \sigma$-out and π-in $\rightarrow G_\sigma \rightarrow \pi$-out. However, the latter process is found to be 10^5 times larger than the former. It is stressed that the cross-conjugated molecules are fully conjugated from the central part of the molecule and to the left and right electrodes, respectively, but not from electrode to electrode.[33] Therefore, it seems reasonable that the overtone processes where both the in-channel and the out-channel are from the high-transmission fully conjugated π-system, and where the antiresonance is bypassed by the dual scattering event, are dominant. When viewing IETS overtone processes in combination with quantum interference, it is therefore not surprising that a large or an even larger overtone peak than for the corresponding fundamental mode can be observed. While it is clear that interference is a necessity for the overtones to be observed, it is unclear which other conditions must be fulfilled in order to obtain overtones larger than the fundamental. This is exemplified by the two seemingly similar modes for CC, the hydrogen wag and the hydrogen twist. Overtone modes are present for both modes, but only the latter overtone is larger than the corresponding fundamental mode.

Model Calculations. In order to illustrate the fundamental difference between linear and cross-conjugated molecules, and to show that the electron−phonon coupling elements need not to be large to reproduce the overtones, a simple model calculation is presented.

First, it is important to understand the form of the electron−phonon coupling matrix in order to know which orbitals are coupled to which by the relevant vibrational modes. In order to do this, the electron−phonon coupling matrix and the Hamiltonian was exported out of gDFTB, transformed into an sp^2 hybrid orbital basis and then orthogonalized. See Supporting Information for details. This is done in order to see which orbitals couple to which orbitals directly. Because of the orthogonalization some locality of the orbitals is lost, implying that they are no longer purely atom centered hybrid orbitals and are not strictly guaranteed to be localized on a single atom. However, the problem is minimal in the present case because of the small basis set used.

Two vibrational modes were chosen, the symmetric C═C stretch mode and the asymmetric wagging mode of the two hydrogens. The former does not give rise to an overtone, whereas the latter does. The gDFTB program utilizes a minimal basis set, with one *s*- and three *p*-orbitals for carbon, one *s*- orbital for hydrogen, and one *s*-, three *p*-, and five *d*-orbitals for sulfur and gold. The electron−phonon coupling matrices for both vibrational modes only have significant terms on the central two carbons and two hydrogens, so the model encompasses only these 10 orbitals.

The electron−phonon coupling matrix was found to contain nonzero coupling between all orbitals in the molecule. However, many of these elements were found not to influence the final result. Thus, only

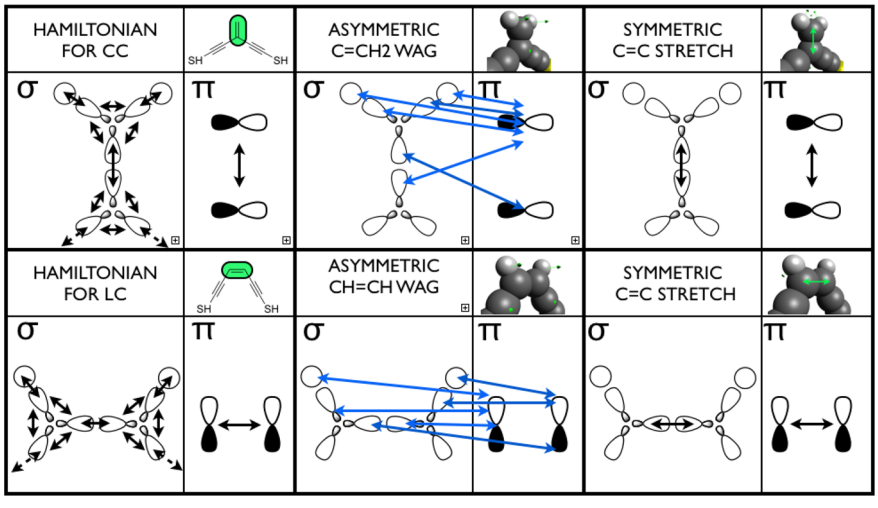

Figure 6. A visualization of the electronic coupling matrix elements of the tight binding Hamiltonian (left) and the electron−phonon matrix for the asymmetric wagging mode (center) and the symmetric carbon−carbon double bond stretch (right) for both CC and LC for the central part of the molecule only The black arrows indicate couplings within the σ- or π-system, whereas the blue arrows indicate couplings between the σ- to the π-system. It is evident that the asymmetric vibrational mode couples the σ- and the π-systems. The force vectors are indicated by the green arrows.

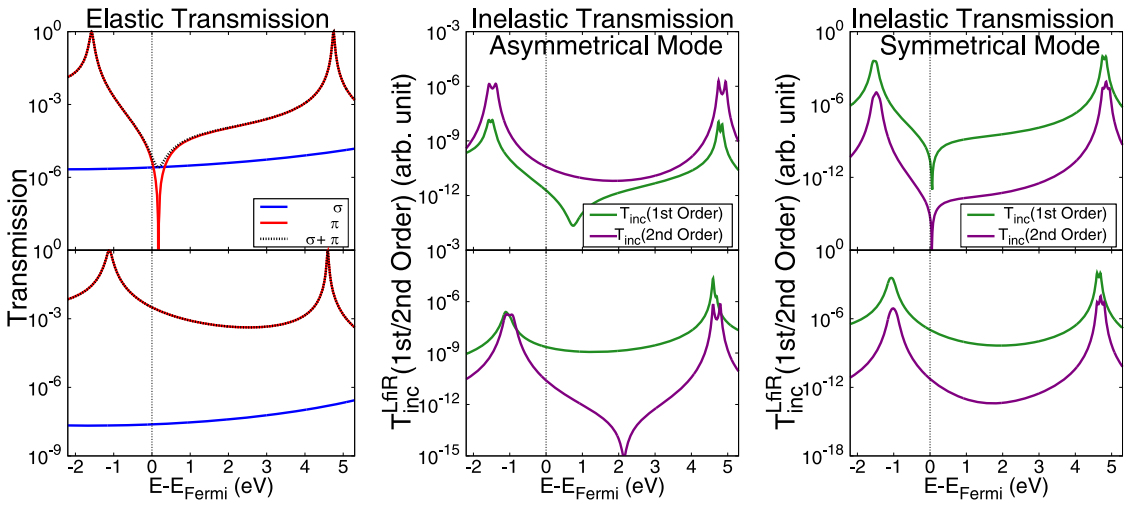

Figure 7. Elastic and inelastic transmissions for CC and LC top and bottom row, respectively. All site energies and coupling strengths are identical for CC and the LC. The only difference between the two Hamiltonians are in the couplings to the hydrogens and to the electrodes, as shown schematically in Figure 6. The elastic transmission (left column) is qualitatively reproduced by the model, with quantum interference for CC and a dominant π-channel for LC. The asymmetric mode (middle column) yields an overtone larger than the fundamental for CC, but not for LC. The inelastic transmission due to the carbon−carbon stretch (right column) shows the fundamental mode dominating for both systems.

the quantitatively important terms in the matrix were retained in order to simplify the analysis of the phenomenon behind the symmetric and the asymmetric scattering processes. For the symmetric mode, the resulting electron−phonon coupling matrix contained only terms that couple the π-orbitals together and terms that couple the σ-orbitals together. For the asymmetric mode, the resulting electron−phonon coupling matrix contained only elements that couple the σ- and the π-subsystems to each other. The form of the electron−phonon coupling matrices are illustrated in Figure 6. Consequently, for the symmetric mode the scattering only occurs within the σ- or the π-system, whereas for the asymmetric mode the resulting terms are those that couple the σ- and the π-channels. An important insight at this stage is that, in order to describe the overtones reported in this paper or asymmetric vibrational modes in general, it is imperative to include both σ- and π-orbitals in the model.

Most model calculations of IETS tend to reduce the size of the Hamiltonian of the interacting region in order to simplify the effect of the various processes studied. Typically, this is done by using only a single site per atom, which in this case would only constitute a model for the π-system. In this case, however, we need a model that encompasses both the σ- and the π-system in order to model the overtones, and consequently the Hamiltonian cannot be further reduced.

On the basis of the form of the electron−phonon coupling matrix, the minimal Hamiltonian must necessarily consist of two carbon atoms and two hydrogens atoms. The site energies and the coupling elements between the sites are taken from the gDFTB Hamiltonian of CC. The overlap between the orbitals was removed by orthogonalizing the gDFTB Hamiltonian, and only the nearest neighbor coupling elements retained. The model system consists of a σ-backbone consisting of three sp^2 hybrid orbitals per carbon and one *s*-orbital per hydrogen and the π-system consists of a *p*-orbital per carbon. The π-system is orthogonal to the σ-backbone. The σ- and the π-systems each couple to the electrodes *via* a single site. This model can be considered as an extension to the model used previously,[48] with parameters taken from the gDFTB Hamiltonian and the addition of an orthogonal σ-system.

The model Hamiltonian matrix for LC was constructed with the same elements as those used in the model Hamiltonian for CC; however, the coupling elements were shuffled in order to reflect the topology of a linearly conjugated molecule. With this model, we can show that the cross conjugation is the key ingredient to obtain overtones in IETS. The orbitals and couplings for the two model Hamiltonians are illustrated in Figure 6.

The inelastic processes behind the overtone are studied in a simple manner by considering the inelastic transmission, T_{inc} (see Supporting Information). The inelastic transmission is a function of energy that must be integrated in order to get the current, similar to the elastic transmission.

To compute the inelastic transmission in the simplest manner possible, the nonrenormalized Green's functions and $\Gamma^{L(R)}$s are used, and the inelastic transmission for the first- and second-order scattering processes are calculated separately.

Since the Hamiltonian consists of orthogonal σ- and π-systems, it is possible to separate the transmission and the inelastic transmission into a sum of symmetry components. The results are shown in Figure 7. It is emphasized that the second overtone and higher

order processes are found to contribute very little (much less than 1%) to the total inelastic transmission.

The inelastic transmission for the symmetric stretch mode for the model of CC and LC is shown in the right column of Figure 7. The inelastic transmission is found to be is proportional to the elastic transmission of the π-system in both cases only reduced by a constant factor. Consequently, an interference feature is observed near the Fermi energy for CC, offering an explanation as to why this mode is suppressed in the IETS of CC. The inelastic transmission of the overtone for both CC and LC are similar in shape to the inelastic transmission of the fundamental, only further reduced. Thus, it seems that the inelastic transmission for symmetric modes falls off exponentially as a function of order in the scattering. This illustrates why symmetric modes in the *main tunneling path* are dominant for molecules with a single dominant elastic transmission channel,[23,24] and why overtones in IETS are rarely observed.

The inelastic transmission for the asymmetric hydrogen twist mode is shown in the central column of Figure 7, and the results differ significantly from the results for the symmetric mode. The inelastic transmissions are, for this mode, not proportional to the elastic transmission, and the second-order scattering is larger for the cross-conjugated CC. The second-order scattering for LC is found to be much smaller than the first-order scattering process at the Fermi energy. Interestingly, an interference feature in the inelastic transmission is observed for CC in the first-order scattering and for LC in the second-order scattering. The origin of this behavior is not understood. It is emphasized that the parameters in the Hamiltonians of CC and LC are identical except for the connectivity of the orbitals. It is thereby shown that the overtone can be recreated in a simple model system. It is furthermore shown that the overtone does not require unusual parameters and that the interference feature is a key ingredient.

The expression for inelastic transmission for symmetric modes are essentially found by multiplication of matrices of the relevant elastic channels $A_{L/R}$ and the electron−phonon coupling matrix α_{qsym} (see eq 1). The elastic channels reduce to the submatrices due to the dominant transmission channel since there is no scattering between different elastic channels. The higher order scattering processes are simply given by more of the same matrices multiplied together, eq 2, and since the multiplication of these matrices gives something smaller than 1, the inelastic transmission must decrease uniformly as a function of scattering order.

For asymmetric vibrational modes, on the other hand, the expressions for the first-order and second-order scattering processes are fundamentally different, since the first-order process is described by scattering between the elastic channels of the π- and the σ-system, whereas the second-order scattering involves the elastic channels of the π-system only. Consequently, the inelastic transmission is not uniformly decreasing as a function of scattering order and allows for overtone processes since the π-channels are generally more transmissive than the σ-channels, even in systems where the fundamental mode is allowed and significant.

CONCLUSIONS

We have studied the inelastic contributions to the current in cross-conjugated molecules. We find that the inelastic current constitutes a larger proportion of the total current in cross-conjugated molecules compared with linearly conjugated molecules. However, the inelastic current is not large enough to totally undermine the effect of the destructive interference predicted in these molecules. This finding is supported by recent experimental studies.[1−3] Since the inelastic current is predicted to constitute a much larger proportion of the total current, it seems that cross-conjugated molecules could be suitable probes for IETS studies of various structure−property relationships since the sensitivity in IETS may be significantly improved. Furthermore, using appropriate chemical substitution, it should be possible to increase the ratio of inelastic to elastic current even further.

Second, we predict that overtone modes should be present in IET spectra of cross-conjugated molecules. The calculations are supported by additional studies using a model system with identical parameters, changing only the topology so as to make a linear or a cross-conjugated molecule. The overtones are explained by a scattering mechanism where the incoming electron is scattered from the π-channel to the σ-system and back to the π-system again before exiting out into the right electrode. The current thereby bypasses the interference feature of the cross-conjugated molecules, while still flowing mainly in the high-transmission π-channel. This dual scattering mechanism turns out to be more favorable since the electrons are allowed to flow primarily through the high transmission π-system. Whether this process is observed in all molecules that exhibit quantum interference, or different classes of quantum interference exist, remains to be seen.

In the computations, it is easy to show that a single vibrational mode results in two peaks in the IET spectra, simply by including only a single vibrational mode in the calculation. In experiments it is a more difficult problem, since the overtone can be hidden behind other peaks in the spectrum or because the overtone process are energetically close to another fundamental mode making it difficult to know which vibrational modes are observed in the IET spectrum. However, it should be possible to unambiguously show that overtone processes are in fact being observed by using isotopic substitutions.[39] The energy of the vibrational modes depend on, among other things, the

mass of the atoms involved, and substituting the hydrogens to deuterium will shift the fundamental modes by one quantum of energy and the overtones modes by two.

METHODS

In order to calculate the IET spectra, the molecules are optimized between two Au(111) surfaces. The molecular geometry optimization is started at the fcc hollow site 2.64 Å above the surface. This surface−sulfur distance is obtained by optimizing the molecule above a single Au(111) surface. The overtones in the IET spectra are found to be relatively insensitive to the size of the Au electrodes (see Supporting Information Figure S2) and to changes in the gold−thiolate distance where the overtone modes are clearly visible for distances between 2 and 3 Å between the thiolate and the Au surface. The IET spectra change significantly at very small Au−sulfur distances, where the molecule is far away from its (vacuum) equilibrium structure and where the interference effects are no longer present (see Supporting Information Figure S3). Periodic boundary conditions are used in the planes perpendicular to the Au−molecule−Au axis. Both the geometries and the vibrational modes are computed using scc-DFTB.[49−51] The transport calculations are performed using the gDFTB program, which combines SCC-DFTB with the Green's function formalism.[52,53] The electron−phonon interaction is included *via* the Born approximation[42,52,54] (see Supporting Information) up to third order, which in this case corresponds to a converged solution (see Supporting Information Figure S4).

While the method is certainly cheap computationally because of the parametrized tight-binding approach, it has also been shown to yield good results compared with experiments,[26] as have other similar density functional theory-based methods,[27,55] illustrating that electron−phonon interactions in organic molecules are treated with reasonable accuracy. This probably stems from the fact that the electron−phonon couplings are closely connected to the ground state geometry of the molecule, a problem treated well within the DFT framework.

Conflict of Interest: The authors declare no competing financial interest.

Acknowledgment. The research leading to these results has received funding from the European Research Council under the European Union's Seventh Framework Program (FP7/2007-2013)/ERC Grant Agreement No. 258806.

Supporting Information Available: Full description of the formalism used to calculate IETS, symmetry resolved IETS, control calculations varying the geometry, and all details of the parameters used in the model calculations. This material is available free of charge *via* the Internet at http://pubs.acs.org/.

REFERENCES AND NOTES

1. Guedon, C. M.; Valkenier, H.; Markussen, T.; Thygesen, K. S.; Hummelen, J. C.; van der Molen, S. J. Observation of Quantum Interference in Molecular Charge Transport. *Nat. Nanotechnol.* **2012**, *7*, 305–309.
2. Hong, W.; Valkenier, H.; Mészáros, G.; Manrique, D. Z.; Mishchenko, A.; Putz, A.; García, P. M.; Lambert, C. J.; Hummelen, J. C.; Wandlowski, T. An MCBJ Case Study: The Influence of Π-Conjugation on the Single-Molecule Conductance at a Solid/Liquid Interface. *Beilstein J. Nanotechnol.* **2011**, *2*, 699–713.
3. Arroyo, C. R.; Tarkuc, S.; Frisenda, R.; Seldenthuis, J. S.; Woerde, C. H. M.; Eelkema, R.; Grozema, F. C.; va1 de1 Zant, H. S. J. Signatures of Quantum Interference Effects on Charge Transport through a Single Benzene Ring. *Angew. Chem., Int. Ed.* **2013**, *125*, 3234–3237.
4. Andrews, D. Q.; Solomon, G. C.; Van Duyne, R. P.; Ratner, M. A. Single Molecule Electronics: Increasing Dynamic Range and Switching Speed Using Cross-Conjugated Species. *J. Am. Chem. Soc.* **2008**, *130*, 17309–17319.
5. Reed, M. A.; Zhou, C.; Muller, C. J.; Burgin, T. P.; Tour, J. M. Conductance of a Molecular Junction. *Science* **1997**, *278*, 252–254.
6. Di Ventra, M.; Pantelides, S. T.; Lang, N. D. First-Principles Calculation of Transport Properties of a Molecular Device. *Phys. Rev. Lett.* **2000**, *84*, 979–982.
7. Solomon, G. C.; Gagliardi, A.; Pecchia, A.; Frauenheim, T.; Di Carlo, A.; Reimers, J. R.; Hush, N. S. Molecular Origins of Conduction Channels Observed in Shot-Noise Measurements. *Nano Lett.* **2006**, *6*, 2431–2437.
8. Sergueev, N.; Tsetseris, L.; Varga, K.; Pantelides, S. Configuration and Conductance Evolution of Benzene-Dithiol Molecular Junctions under Elongation. *Phys. Rev. B: Condens. Matter Mater. Phys.* **2010**, *82*, 073106.
9. Emberly, E. G.; Kirczenow, G. Theoretical Study of Electrical Conduction through a Molecule Connected to Metallic Nanocontacts. *Phys. Rev. B: Condens. Matter Mater. Phys.* **1998**, *58*, 10911–10920.
10. Emberly, E. G.; Kirczenow, G. Models of Electron Transport through Organic Molecular Monolayers Self-Assembled on Nanoscale Metallic Contacts. *Phys. Rev. B: Condens. Matter Mater. Phys.* **2001**, *64*, 235412.
11. Strange, M.; Rostgaard, C.; Häkkinen, H.; Thygesen, K. S. Self-Consistent GW Calculations of Electronic Transport in Thiol- and Amine-Linked Molecular Junctions. *Phys. Rev. B: Condens. Matter Mater. Phys.* **2011**, *83*, 115108.
12. Häkkinen, H. The Gold-Sulfur Interface at the Nanoscale. *Nat. Chem.* **2012**, *4*, 443–455.
13. Lin, L.-L.; Zou, B.; Wang, C.-K.; Luo, Y. Assignments of Inelastic Electron Tunneling Spectra of Semifluorinated Alkanethiol Molecular Junctions. *J. Phys. Chem. C* **2011**, *115*, 20301–20306.
14. Jaklevic, R. C.; Lambe, J. Molecular Vibration Spectra by Electron Tunneling. *Phys. Rev. Lett.* **1966**, *17*, 1139–1140.
15. Wang, W.; Lee, T.; Kretzschmar, I.; Reed, M. A. Inelastic Electron Tunneling Spectroscopy of an Alkanedithiol Self-Assembled Monolayer. *Nano Lett.* **2004**, *4*, 643–646.
16. Kushmerick, J. G.; Lazorcik, J.; Patterson, C. H.; Shashidhar, R.; Seferos, D. S.; Bazan, G. C. Vibronic Contributions to Charge Transport across Molecular Junctions. *Nano Lett.* **2004**, *4*, 639–642.
17. Hihath, J.; Bruot, C.; Tao, N. Electron-Phonon Interactions in Single Octanedithiol Molecular Junctions. *ACS Nano* **2010**, *4*, 3823–3830.
18. Bruot, C.; Hihath, J.; Tao, N. Mechanically Controlled Molecular Orbital Alignment in Single Molecule Junctions. *Nat. Nanotechnol.* **2012**, *7*, 35–40.
19. Yu, L. H.; Zangmeister, C. D.; Kushmerick, J. G. Origin of Discrepancies in Inelastic Electron Tunneling Spectra of Molecular Junctions. *Phys. Rev. Lett.* **2007**, *98*, 206803.
20. Gagliardi, A.; Solomon, G. C.; Pecchia, A.; Frauenheim, T.; Di Carlo, A.; Hush, N. S.; Reimers, J. R. *A Priori* Method for Propensity Rules for Inelastic Electron Tunneling Spectroscopy of Single-Molecule Conduction. *Phys. Rev. B: Condens. Matter Mater. Phys.* **2007**, *75*, 174306.
21. Hipps, K. W.; Aplin, A. T. The Tricyanomethanide Ion: An Infrared, Raman, and Tunneling Spectroscopy Study Including Isotopic Substitution. *J. Phys. Chem.* **1985**, *89*, 5459–5464.
22. Hipps, K. W. Tunneling Spectroscopy of Organic Monolayers and Single Molecules. *Unimolecular and Supramolecular Electronics II*; Metzger, R. M., Ed.; Springer: Berlin, **2012**; pp 189−215.
23. Troisi, A.; Ratner, M. A. Molecular Transport Junctions: Propensity Rules for Inelastic Electron Tunneling Spectra. *Nano Lett.* **2006**, *6*, 1784–1788.
24. Troisi, A.; Ratner, M. A. Propensity Rules for Inelastic Electron Tunneling Spectroscopy of Single-Molecule Transport Junctions. *J. Chem. Phys.* **2006**, *125*, 214709–214711.

25. Paulsson, M.; Frederiksen, T.; Ueba, H.; Lorente, N.; Brandbyge, M. Unified Description of Inelastic Propensity Rules for Electron Transport through Nanoscale Junctions. *Phys. Rev. Lett.* **2008**, *100*, 226604.
26. Solomon, G. C.; Gagliardi, A.; Pecchia, A.; Frauenheim, T.; Di Carlo, A.; Reimers, J. R.; Hush, N. S. Understanding the Inelastic Electron-Tunneling Spectra of Alkanedithiols on Gold. *J. Chem. Phys.* **2006**, *124*, 094704–094710.
27. Paulsson, M.; Frederiksen, T.; Brandbyge, M. Inelastic Transport through Molecules: Comparing First-Principles Calculations to Experiments. *Nano Lett.* **2006**, *6*, 258–262.
28. Troisi, A.; Beebe, J. M.; Picraux, L. B.; van Zee, R. D.; Stewart, D. R.; Ratner, M. A.; Kushmerick, J. G. Tracing Electronic Pathways in Molecules by Using Inelastic Tunneling Spectroscopy. *Proc. Natl. Acad. Sci. U. S. A.* **2007**, *104*, 14255–14259.
29. Kirtley, J.; Soven, P. Multiple-Scattering Theory of Intensities in Inelastic-Electron-Tunneling Spectroscopy. *Phys. Rev. B: Condens. Matter Mater. Phys.* **1979**, *19*, 1812–1817.
30. Solomon, G. C.; Andrews, D. Q.; Van Duyne, R. P.; Ratner, M. A. When Things Are Not as They Seem: Quantum Interference Turns Molecular Electron Transfer "Rules" Upside Down. *J. Am. Chem. Soc.* **2008**, *130*, 7788–7789.
31. Solomon, G. C.; Herrmann, C.; Vura-Weis, J.; Wasielewski, M. R.; Ratner, M. A. The Chameleonic Nature of Electron Transport through Π-Stacked Systems. *J. Am. Chem. Soc.* **2010**, *132*, 7887–7889.
32. Ke, S.-H.; Yang, W.; Baranger, H. U. Quantum-Interference-Controlled Molecular Electronics. *Nano Lett.* **2008**, *8*, 3257–3261.
33. Phelan, N. F.; Orchin, M. Cross Conjugation. *J. Chem. Educ.* **1968**, *45*, 633.
34. Solomon, G. C.; Gagliardi, A.; Pecchia, A.; Frauenheim, T.; Di Carlo, A.; Reimers, J. R.; Hush, N. S. The Symmetry of Single-Molecule Conduction. *J. Chem. Phys.* **2006**, *125*, 184702–184705.
35. Meir, Y.; Wingreen, N. S. Landauer Formula for the Current through an Interacting Electron Region. *Phys. Rev. Lett.* **1992**, *68*, 2512–2515.
36. Solomon, G. C.; Herrmann, C.; Hansen, T.; Mujica, V.; Ratner, M. A. Exploring Local Currents in Molecular Junctions. *Nat. Chem.* **2010**, *2*, 223–228.
37. Fracasso, D.; Valkenier, H.; Hummelen, J. C.; Solomon, G. C.; Chiechi, R. C. Evidence for Quantum Interference in SAMs of Arylethynylene Thiolates in Tunneling Junctions with Eutectic Ga-in (Egain) Top-Contacts. *J. Am. Chem. Soc.* **2011**, *133*, 9556–9563.
38. Darwish, N.; Díez-Pérez, I.; Da Silva, P.; Tao, N.; Gooding, J. J.; Paddon-Row, M. N. Observation of Electrochemically Controlled Quantum Interference in a Single Anthraquinone-Based Norbornylogous Bridge Molecule. *Angew. Chem., Int. Ed.* **2012**, *51*, 3203–3206.
39. Stipe, B. C.; Rezaei, M. A.; Ho, W. Single-Molecule Vibrational Spectroscopy and Microscopy. *Science* **1998**, *280*, 1732–1735.
40. Chen, Y.-C.; Zwolak, M.; Di Ventra, M. Inelastic Current-Voltage Characteristics of Atomic and Molecular Junctions. *Nano Lett.* **2004**, *4*, 1709–1712.
41. Makk, P.; Tomaszewski, D.; Martinek, J.; Balogh, Z.; Csonka, S.; Wawrzyniak, M.; Frei, M.; Venkataraman, L.; Halbritter, A. Correlation Analysis of Atomic and Single-Molecule Junction Conductance. *ACS Nano* **2012**, *6*, 3411–3423.
42. Pecchia, A.; Di Carlo, A.; Gagliardi, A.; Sanna, S.; Frauenheim, T.; Gutierrez, R. Incoherent Electron-Phonon Scattering in Octanethiols. *Nano Lett.* **2004**, *4*, 2109–2114.
43. Sols, F.; Macucci, M.; Ravaioli, U.; Hess, K. On the Possibility of Transistor Action Based on Quantum Interference Phenomena. *Appl. Phys. Lett.* **1989**, *54*, 350–352.
44. Song, H.; Reed, M. A.; Lee, T. Single Molecule Electronic Devices. *Adv. Mater.* **2011**, *23*, 1583–1608.
45. Okabayashi, N.; Paulsson, M.; Ueba, H.; Konda, Y.; Komeda, T. Inelastic Tunneling Spectroscopy of Alkanethiol Molecules: High-Resolution Spectroscopy and Theoretical Simulations. *Phys. Rev. Lett.* **2010**, *104*, 077801.
46. Song, H.; Kim, Y.; Ku, J.; Jang, Y. H.; Jeong, H.; Lee, T. Vibrational Spectra of Metal-Molecule-Metal Junctions in Electromigrated Nanogap Electrodes by Inelastic Electron Tunneling. *Appl. Phys. Lett.* **2009**, *94*, 103110–103113.
47. It should be noted that the virtual state is not a channel in the sense discussed above, but rather a retarded Green's function. Nevertheless, it still transforms with σ-like properties, *i.e.*, unchanged by the mirror operation.
48. Solomon, G. C.; Andrews, D. Q.; Hansen, T.; Goldsmith, R. H.; Wasielewski, M. R.; Van Duyne, R. P.; Ratner, M. A. Understanding Quantum Interference in Coherent Molecular Conduction. *J. Chem. Phys.* **2008**, *129*, 054701–054708.
49. Porezag, D.; Frauenheim, T.; Köhler, T.; Seifert, G.; Kaschner, R. Construction of Tight-Binding-Like Potentials on the Basis of Density-Functional Theory: Application to Carbon. *Phys. Rev. B: Condens. Matter Mater. Phys.* **1995**, *51*, 12947–12957.
50. Seifert, G.; Porezag, D.; Frauenheim, T. Calculations of Molecules, Clusters, and Solids with a Simplified LCAO-DFT-LDA Scheme. *Int. J. Quantum Chem.* **1996**, *58*, 185–192.
51. Elstner, M.; Porezag, D.; Jungnickel, G.; Elsner, J.; Haugk, M.; Frauenheim, T.; Suhai, S.; Seifert, G. Self-Consistent-Charge Density-Functional Tight-Binding Method for Simulations of Complex Materials Properties. *Phys. Rev. B: Condens. Matter Mater. Phys.* **1998**, *58*, 7260–7268.
52. Pecchia, A.; Carlo, A. D. Atomistic Theory of Transport in Organic and Inorganic Nanostructures. *Rep. Prog. Phys.* **2004**, *67*, 1497.
53. Frauenheim, T.; Seifert, G.; Elstner, M.; Niehaus, T. A.; Köhler, C.; Amkreutz, M.; Sternberg, M.; Hajnal, Z.; Carlo, A. D.; Suhai, S. Atomistic Simulations of Complex Materials: Ground-State and Excited-State Properties. *J. Phys.: Condens. Matter* **2002**, *14*, 3015.
54. Gagliardi, A.; Romano, G.; Pecchia, A.; Di Carlo, A.; Frauenheim, T.; Niehaus, T. A. Electron-Phonon Scattering in Molecular Electronics: From Inelastic Electron Tunneling Spectroscopy to Heating Effects. *New J. Phys.* **2008**, *10*, 065020.
55. Lin, L.-L.; Wang, C.-K.; Luo, Y. Inelastic Electron Tunneling Spectroscopy of Gold-Benzenedithiol-Gold Junctions: Accurate Determination of Molecular Conformation. *ACS Nano* **2011**, *5*, 2257–2263.